A Multiple Snow Layer Model Including a Parameterization of Vertical Water Channel Process in Snowpack

Takafumi KATSUSHIMA[a]*, Toshiro KUMAKURA[a], and Yukari TAKEUCHI[b]
[a]Nagaoka University of Technology, Nagaoka, Niigata, JAPAN
[b]Tohkamachi Experimental Station, Forestry and Forest Products Research Institute, Tohkamachi, Niigata, JAPAN

ABSTRACT: Tohkamachi Experimental Station in Niigata prefecture, Japan, which locates along Sea of Japan, usually has heavy snow in winter. In this site, much snow melting water and rain are observed in middle winter, because it has higher temperature than other cold regions. Then, there is much vertical water infiltrations which go through the water channel formed in the snowpack.
In this study, we attempt to implement new parameterization of the water channel process in our multiple snow layer model, which already has the infiltration process with the Darcy's law, to validate vertical water fluxes at each snow layers. We found that the result in our model with new parameterization is better agreement with the observation than the result without the water channel processes.

KEYWORDS: preferential flow, water channel, parameterization, multiple snow layer model

1. INTRODUCTION

Preferential flow in snowpack is an important process to study the avalanche forecast and runoff below snowpack. It is also important to reproduce weak layers and profiles of the hardness, snow temperature and snow density in the snowpack using numerical models for these purposes. On the other hand, the preferential flow occurs in dry snow maintained in the middle of snowpack, which is penetrated by the infiltration of liquid water. Thus, it is thought that a process of the preferential flow is essential to simulate the physical properties of the snowpack realistically (Gustafsson et al., 2004).

In colder region, the rainfall and meltwater usually occurred in spring and early summer. In warmer region such as Hokuriku district in JAPAN, it occurs in middle winter, and water channels are formed as a result of the water flow. For this reason, the water channel is observed in middle-winter snowpack in Japan; e.g., Nohguchi (1984); Takeuchi et al. (2007).

However, already-developed infiltration models for the snowpack are simple models to assume an uniform flow; e.g., Jordan (1991); Brun (1992); Lehning et al. (1999).

The past models to calculate the infiltration into the snow pack have not considered the preferential flow; e.g., Colbeck (1972, 1974, and 1977); Jordan (1983); Illangasekave et al. (1990); Pfeffer et al. (1990). Marsh and Woo (1984a, 1984b) used averaged fraction of the preferential flow over horizontal area to calculate positions of wetting fronts and the runoff in the snowpack by the preferential flow. Colbeck (1979) proposed a multi flow path model to calibrate water fluxes in the snow. But, it did not predict the lateral flow and the preferential flow in the model because these models expressed the snowpack as one layer vertically.

It is known that the lateral flow and the preferential flow form on/below impermeable layers. And the impermeable layers form in the following three situations. 1) On a boundary layer which forms below a fine textured layer and above a coarse textured layer; e.g., Wakahama (1963); Waldner et al. (2004). 2) On a boundary which forms below snow layer and above ice layer; e.g., Gerbel (1954); Langham (1974); Marsh and Woo (1984a, 1984b). 3) On a wetting front into dry snow layer; e.g., Nohguchi (1984). But, the modeling studies of it have not become active because the physical theories for the formation of the preferential flow have not become clear yet.

In this study, we attempt to develop a new parameterization of the preferential flow or water channel processes in our snow layer model, which has the infiltration process with the Darcy's law, to validate vertical water fluxes at each snow layers.

2. STUDY SITE

In this study, we use the meteorological data observed in Tohkamachi Experimental Station, Forestry and Forest Products Research Institute (37°08'N, 138°46'E, 200m a.s.l.) in

* *Corresponding author address:* Takafumi Katsushima, Nagaoka University of Technology, 1603-1 Kamitomioka,Nagaoka,Niigata,JAPAN 940-2188;tel:+81-258-47-1611;email: katusima@hydro.nagaokaut.ac.jp

Niigata, Japan. This site is located along a mountainous valley run down to Sea of Japan (Figure 1). It has much snow in winter and the maximum snow depth is observed more than 2m annually although air temperature is high, which is observed -0.3 degree Celsius of monthly-averaged air temperature from 1918 to 1997 in January and 0.0 degree in February (Yamanoi et al., 2000). In this site, the snowmelt and the rainfall often occur in meddle winter. The snow temperature in the snowpack generally is 0 degree or near 0 degree, because of the snowfall in the situation of air temperature near 0 degree and the following warm days.

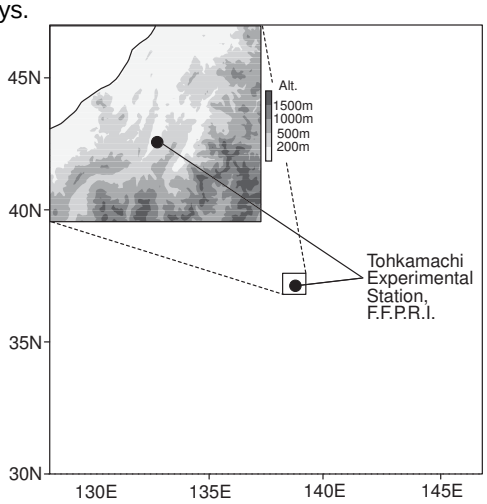

Figure 1: The location of Tohkamachi Experimental Station as the study site.

3. METHOD

We attempt to implement a new model parameterized for the water channel process in our snow layer model (Kumakura et al., 2004), which is a one-dimensional model and has multiple snow layers as vertical expression of the snowpack. We also compare the vertical structures of snowpack between the results of observation and those of calculation, which are assumed uniform condition with Darcy's low and non-uniform condition using the parameterization of the preferential flow snow.

We use the data observed in 2005/06, when we have heavy snow along Sea of Japan in those years. Takeuchi et al. (2007) descried detail of pit observations in 2005/06 winter at Tohkamachi Experimental Station and reported the occurrence of the water channel and the dimple at the snow surface caused by the infiltration into dry snow from the pit observation in 16 January, 2006.

The input metrological data into the model are hourly data of precipitation, air temperature, humidity, wind speed, net radiation and heat flux to the soil near ground. The following observation data are used for comparing with the results of the model outputs. These are snow depth, SWE(Snow Water Equivalent) with a snow weight measurement instrument (metal wafer type), runoff into the soil with a lysimeter (3.6m×3.6m), SWE with a snow sampler, which is observed in every day not in holiday, and the snow pit observations about 10 days interval.

3.1 MODEL DESCRIPTION

Our model; e.g. Kumakura et al. (2004) is considered the processes of the snowfall, the settlement and the snowmelt. Originally this model has the snowmelt process based on the degree-day method at the snow surface, but now a heat balance method is employed as a realistic heat process It is also changed that the model newly employs the heat flux from the soil for snow melting at a ground/snow interface, a new formula for compactive viscosity coefficients to calculate settlement in dry and wet conditions, and the simple infiltration process using a threshold value of a maximum liquid water content to control the occurrence of the infiltration (last one is not used in this report). By the way, a heat transport process in the snowpack is neglected because the snow temperature in whole of snowpack generally has temperature 0 degree.

At first, we implement the uniform infiltration process with the Darcy's law before the new parameterization of the preferential flow process and a snow metamorphism process to calculate average diameter are implemented.

SNOWFALL PROCESS

A weight of new snow estimates from the precipitation observed with a precipitation gauge. The precipitation type, i.e. liquid precipitation and solid precipitation, discriminates by a wet bulb temperature. The depth of new snow is calculated with a empirical formula. And we correct the weight of the observed precipitation using a catch ratio of the precipitation gauge (Yokoyama et al., 2003).

We use the wet bulb temperature T_w for the discrimination between the liquid precipitaion and the solid precipitation. T_w= 0 degree is used as a threshold value for the discrimination.

$$T_w = T_a - \frac{\varepsilon L}{c_p p}(e_s - e) \qquad (1)$$

where T_a is an air temperature(K), p is an air pressure(Pa), R_h is a relative humidity, e_s is a saturated vapor pressure(Pa) and e is a vapor pressure(Pa). The saturated vapor pressure at a ice surface e_s(Pa) is calculated with the following formula obtained by Sonntag(1994).

$$e_s = 100 \times \exp(-6024.5282 T_a^{-1} + 24.721994 + 1.0613868 \times 10^{-2} T_a - 1.3198825 \times 10^{-5} T_a^{2} - 0.49382577 \ln T_a) \quad (2)$$

It is known that the weight of the precipitation observed with the normal precipitation gage is smaller than the true precipitation. When wind strongly blows, the particles of the precipitation caught by the gauge tend to decrease. This ratio, which is usually called catch ratio, between the measured and true precipitation of the solid hydrometeor is more remarkable than that of liquid. Then we need to correct the observed precipitation using the catch ratio C_R which is obtained by Yokoyama et al. (2003) and the formula is following,

$$C_R = \frac{1}{1 + m w_s} \quad (3)$$

where w_s is a wind speed (m s^{-1}), m is a coefficient which is different in the precipitation types and the gauge types. The gauge type we used is so called RT-4 (over flow type gauge with wind shelter), and the coefficient m of this gauge is 0.128 for the snow and 0.0192 for the rain.

We use the following formula of new snow density ρ_0 (kg m^{-3}) which is obtained by Hirai et al. (2007) estimated from field observations performed by Kajikawa (1989).

$$\rho_0 = 3.6 w_s - 0.2 T_a + 62 \quad (4)$$

SNOWMELT PROCESS

Snow melt is calculated with the heat balance method at the snow surface and the ground interface.

A heat balance equation at the snow surface is given as

$$M_s = R_n + Q_s + Q_l + Q_r + Q_u \quad (5)$$

where M_s is a snowmelt heat flux, R_n is a net radiation, Q_s is a sensible heat flux, Q_l is a latent heat flux, Q_r is a heat flux from the rain, Q_u is a heat flux into snowpack. The net radiation is directly used from observation data with a net radiometer, but other fluxes are estimated from other kinds of the data of meteorological observations. We neglect the heat transport process as mentioned above and assume the heat flux in the snowpack is Q_u=0.

The sensible heat flux Q_s and the latent heat flux Q_l is estimated using a following bulk method.

$$Q_s = c_p \rho_a C (T_a - T_s) \quad (6)$$

where c_p is a specific heat at the constant pressure in dry air, ρ_a is an air density(kg m^{-1}), C is a bulk transfer coefficient (m s^{-1}), T_a(K) is the air temperature in height of z_a, T_s(K) is a snow surface temperature.

$$Q_l = C \frac{0.622 L \rho_a \beta}{R_a T_a} (e - e_s) \quad (7)$$

where L is the latent heat constant of vaporization from the ice to the water, β is surface moisture availability (we assumed β=1.0 in the snow surface), R_a is gas constant of dry air. On the ice surface,

$$\rho_a = 1.293 \frac{273.15}{T_a} \frac{p}{p_0} (1 - 0.378 \frac{e}{p}) \quad (8)$$

is used, where, p is air pressure which is assumed a constant value of p=9800 (Pa) according to the height of study site, p_0 is the standard pressure p_0 =101325 (Pa). The bulk coefficient is given as

$$C = \frac{k u_*}{0.74 \ln(z_a / z_0)} \quad (9)$$

where k is the Karman constant, u_* is a friction velocity. When the atmospheric stability is neutral,

$$u_* = \frac{k U_a}{\ln(z_a / z_0)} \quad (10)$$

can be used, where Z_a is a height (m) of the wind speed measurement, U_a is a wind speed(m s^{-1}) in the hight of Z_a, Z_0 is an aerodynamic roughness (m) which is use a constant value Z_0=0.0002 assuming the snow surface. The heat flux from the rain is given as

$$Q_r = r_r c_{pw} (T_a - T_s) \quad (11)$$

where r_r is rain fall intensity (kg m^{-2} s^{-1}), c_{pw} is specific heat of water at the constant pressure.

The heat balance equation at the ground interface is given as

$$M_g = Q_g + Q_u \quad (12)$$

where M_g is a heat flux for snowmelt at the bottom of snowpack, Q_u is an outgoing heat flux from snowpack, Q_g is an incoming heat flux from the ground. In our model, we neglect Q_u because of the constant temperature of whole snowpack. Thus, the snow melt at the ground interface is just estimated from Q_g.

SETTLEMENT PROCESS

The viscous compression of snow layers is calculate

$$\frac{dh}{dt} = -\frac{\sigma}{\eta} h \tag{13}$$

where $h(\mathrm{m})$ is a layer thickness, σ is a downward load (Pa) of an overburdened snow, η is the compactive viscosity $(\mathrm{Pa\ s})$ of the snow. The compactive viscosity is changed according to a kind of a media, i.e. the dry snow or the wet snow.

The compactive viscosity of the dry snow η_d is calculated with a following formula by Shinojima (1967).

$$\eta_d = \eta_0 e^{0.0253\rho - 0.0958T} \tag{14}$$

where η_0 is 3.44×10^6 $(\mathrm{Pa\ s})$.

The compactive viscosity of the wet snow η_w is given as the empirical formula by Hirai et al. (2007) which is obtained from the wet snow viscosity measured by Kinosita (1963). That is,

$$\begin{cases} \eta_w = \eta_d e^{-0.092\theta_{vol.wat.}} & (\rho_{dry} \le 400\,\mathrm{kg\,m^{-3}}) \\ \eta_w = \eta_d & (\rho_{dry} > 400\,\mathrm{kg\,m^{-3}}) \end{cases} \tag{15}$$

where $\theta_{vol.wat.}$ is a volumetric liquid water content(%),and ρ_{dry} is the dry snow density $(\mathrm{kg\ m^{-3}})$.

SNOW METAMORPHISM PROCESS

We need to consider the snow metamorphism in the model to calculate an averaged size of snow particles. Then, we consider an equilibrium growth metamorphism and a wet snow metamorphism. On the other hand a kinetic growth metamorphism is neglected because the snow temperature is usually 0 degree, and a depth hoar and a faceted ice crystal is not usually observed in our study site.

We use equations of Brun (1989) and Tusima (1978) for the wet snow metamorphism. Brun (1989) measured the growth rate of the averaged diameter of the snow particles in a condition where a gravimetric liquid water content $\theta_{weight\ wat.}$ (%) ranges from 0% to 10%. Then, they obtained a following formula.

$$\frac{dv}{dt} = 1.28 \times 10^{-8} + 4.22 \times 10^{-10} \theta_{weight\ wat.}{}^3 \tag{17}$$

v is the volume of the ice particle $(\mathrm{mm^3})$, $\frac{dv}{dt}$ is the growth rate of the ice particle$(\mathrm{mm^3\ s^{-1}})$.
On the other hand, Tusima (1978) measured in a condition of the snow immersed in the liquid water and kept the temperature at 0 degree.

$$\frac{d\bar{\phi}}{dt} = \frac{2.5 \times 10^{-4}}{\bar{\phi}^2} \times \frac{1}{3600} \tag{18}$$

where $\bar{\phi}$ is the averaged diameter(mm), $\frac{d\bar{\phi}}{dt}$ is the growth rate of the ice particle$(\mathrm{mm^3\ s^{-1}})$.

According to these studies, we use equation (17) when $\theta_{weight\ wat.}$ ranges from 0% to 10%, and we assume a small one of equation (17) or equation (19) as the maximum growth rate when $\theta_{weight\ wat.}$ is greater than 10%.

For the equilibrium growth metamorphism, we use e.q. (16) as the weight liquid water content in equation (16) is $\theta_{weight\ wat.}$ =0%.

$$\frac{dv}{dt} = 1.28 \times 10^{-8} \tag{19}$$

A method for obtaining an initial value of the averaged diameter is referred to the method developed by Brun et al. (1992) and we decide to use 0.1mm for the initial values.

At the result of this study, we need to define the dry snow and the wet one. We decide to the snow type in the model as follows. The dry snow, namely “rounded snow”, has the liquid water content as 0 and the wet snow, namely “wet grains”, has it as larger than 0.

3.2 INFILTRATION PROCESSES

As mentioned above, we take into account of the Darcy’s law as the uniform infiltration process under isothermal conditions in our model, based on the energetic studies of Colbeck (1972, 1974, and 1977). After that, we attempt to implement the new parameterization of the infiltration process of the preferential flow due to the water channel.

The numerical model to prognosticate the state of the vertical structure in the snowpack which includes any processes of the preferential flow has not been developed yet. Thus, we need to develop the new method to estimate the impermeable layer, the lateral flow and the preferential flow for our model.

Because the model is necessary to represent the impermeable layer due to capillary barriers at the boundary layer between the upper fine textured layer and the under coarse textured layer, the relationship between a capillary pressure and a liquid water saturation (S_w - P_c curve) in each layers is necessary to know. But, S_w - P_c curve is different each other on the snow characteristic; e.g., Coléou et al., 1999; Sugie and Naruse, 2000. In addition, it is difficult to estimate the time dependence of S_w - P_c curve because of the different time-propagation on the metamorphism in each of snow layers.

Generally we also need to know the impermeable process of ice layers as the capillary barrier, which is difficult to reveal for same reason of the formation of impermeable layer at the

boundary between the fine and coarse textured layers. And a melt freeze crust which is formed at the ice layer acts same role as the impermeable layer.

On the other hand, Takeuchi et al. (2007) observed the water channel resulted in the infiltration into the dry snow at early period of the snowy season. Once the water channel is generated, the behavior of the snow layers is dramatically changed from the past one. Therefore, in this early step of the modeling of the water channel process, we consider the water channel which infiltrates into the dry snow, but the water channel due to the fine over curse texture and the ice layer is neglected. In this study, we develop the new parameterization of the water channels for infiltrating into the dry snow, based on the study of Nohguchi (1984) for the formation of the water channel in almost the same condition.

We descried the detail of the model about the infiltration process and the new parameterization as follows.

UNIFORM INFILTRATION PROCESS

As the water infiltration calculated based on the Darcy's law by Colbeck (1972), a flux of water F ($\mathrm{ms^{-1}}$) is given as

$$F = -\frac{k_w}{\mu_w}\left(\frac{\partial Pc}{\partial z} + \rho_w g\right) \tag{19}$$

where k_w is an unsaturated permeability ($\mathrm{m^2}$), μ_w is a viscosity (Pa s) of water, P_c is a capillary pressure (Pa), ρ_w is a density ($\mathrm{kg\ m^{-3}}$) of water.

Colbeck (1973) shows the relation between the capillary pressure and the effective liquid water saturation. It follows that

$$Pc = -\frac{43}{S^{*3}} - 380 \tag{20}$$

where S^* is the effective liquid water saturation. We neglect hysteresis according to wetting. S^* is given from the irreducible liquid water saturation S_{wi}, which we use S_{wi} =0.07 now (Coléou and Lesaffre,1998), and a liquid water saturation S_w. The effective liquid water saturation S^* and the liquid water saturation S_w are following.

$$S^* = \frac{S_w - S_{wi}}{1 - S_{wi}} \tag{21}$$

$$S_w = \frac{\theta_{vol.wat.}/100}{1 - \theta_{vol.i.}/100} \tag{22}$$

where $\theta_{vol.wat.}$ is a volumetric liquid water content(%), $\theta_{vol.i.}$ is a volumetric ice content(%).

The saturated permeability k_s ($\mathrm{m^2}$) is given as follows by Shimizu (1970).

$$k_s = 0.077\bar{\phi}^2 \exp(-7.8 \times \rho_{dry} / \rho_w) \tag{23}$$

where $\bar{\phi}$ is a average diameter (m), ρ_{dry} is the dry snow density ($\mathrm{kg\ m^{-3}}$). The unsaturated permeability k_w is given as

$$k_w = k_s S^{*\varepsilon} \tag{24}$$

where ε is a coefficient depending on pore size distribution. We use ε=3 from Colbeck and Anderson (1982).

NEW PARAMETERIZATION OF THE PREFERENTIAL FLOW

Nohguchi (1984) suggests that the water channels are formed under the conditions of wetting front going down into the dry snow from field observations. In that study, following two conditions are important to form the water channel.

1) The condition of the wetting front infiltrating into the dry snow.
2) The condition of existing a water-saturated layer above the dry snow which has an ability of forming the wetting front.

On the condition 1), we can identify the layer of wetting front infiltrating into the dry snow, using the vertical profile of the liquid water content in the model. But, on the condition 2), the saturated layer resulted in the wetting front into the homogeneous snow is hard to represent in the model. Moreover the deeply-saturated layer, which can be ignored the first member in a left hand side of the equation (19) because the vertical gradient of the capillary pressure become near zero (Colbeck, 1972), tends toward the steady condition (Illangasekare et al.,1990). In this study, we assumed that the water channel is formed when the condition 1) occurs in the model. The conditions 2) should be forced to ignore for now due to the difficulties, which has been revealed in studies of soil physics. The concept of water channel used in new parameterization is shown in Figure 2.

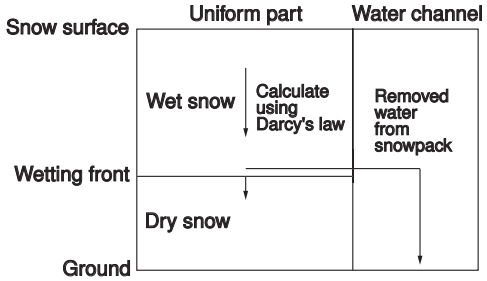

Figure 2: The concept of water channel mechanism used in our model.

The key concept of our water channel model is when the water channel is generated. Then we think that the threshold value of the liquid water content in the wetting front to limit the channel flow is set as the switch of it. After this switch turns on, the water channel is formed immediately and the preferential flow and the lateral flow occur from the wetting front to the ground interface, which is dealt as the removal of the water going through the channel in the model.

The diagnostic procedure of this switch is mentioned below.

$$\begin{cases} S_r = S_0 - S_t \ , S_0 = S_t & (S_0 > S_t) \\ S_r = 0 \qquad\quad , S_0 = S_0 & (S_0 \le S_t) \end{cases} \tag{25}$$

where S_0 is the liquid water saturation at the wetting front, S_t is the threshold value of the liquid water saturation at the wetting front, S_r is the removal of water showing with the unit of the liquid water saturation.The mass of removed water from the wetting front $m_r\,(\mathrm{kg\ m^{-2}})$ is estimated from

$$m_r = S_r \times (100 - \theta_{vol.i.0}) \times \rho_w \times h_0 \tag{26}$$

where $\theta_{vol.i.0}$ is the volumetric ice content(%) in the simulated wetting front, h_0 is the layer thickness at the simulated wetting front.

For deciding the threshold value, we use the fraction of the thickness with the wet grains and calculate a sum of this thickness vertically. The fraction of wet grains layer thickness F_w is

$$F_w = \frac{\sum_{i=1}^{n} h_{wet\,i}}{HS} \tag{27}$$

where h_{wet} is each thickness of the wet grains, n is a number of layers with wet grains, HS is a total depth of the snowpack.

We choose the threshold value from comparing the values of F_w between the observation and the simulation, before obtaining the simulated flux of the uniform infiltration.

4. RESULT

(a) The daily means of the air temperature, (b) the wind speed, (c) the daily total of the rain/snow precipitation which is corrected using the catch ratio for the rain/snow correspondently, (d), (e) the daily total of the simulated snowmelt at the surface and the ground and (f) the daily total of the observed runoff with the lysimeter are shown in Figure 3.The heavy snowfall is observed in December and January and the estimated snowmelt at the snow surface is a little in this period. It is noted that the “rainfall” occurred in January and February. It is thought that we can assume the runoff goes through the water channel because the runoff water is observed after the rainfall immediately. We will mention below in detail.

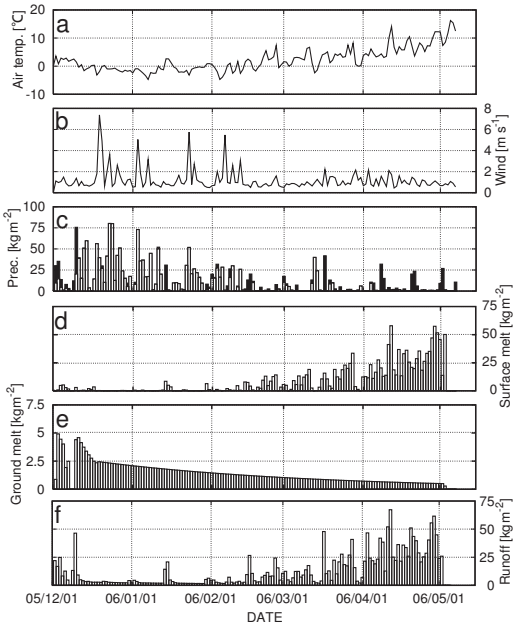

Figure 3: Daily observed and calculated metrological data of a) air temperature, b) wind speed, c) precipitation (the black boxes as the rainfall, the white boxes as the snowfall), d) surface melt, e) ground melt, f) runoff at the ground surface

The observed and simulated snow water equivalent (SWE) and the snow depth are shown in Figure 4. Differences of SWE and the snow depth between the observation, with the snow sampler and the snow depth gauge respectively, and the simulated one are shown in Figure 5. Mean deviations are 63.5(kg m^{-2}) for SWE, 0.25(m) for the snow depth, and Root Mean Square Errors (RMSE) are 78.4(kg m^{-2}) for SWE, 0.31(m) for the snow depth.

The difference of SWE increases at the event of the snowfall starting from the snow accumulation before it becomes about 60 kg m^{-2} in the middle of January (Figure 5). This difference is kept toward the following period with some fluctuation and decreases in the melt season.

Finally, the value of the difference go to zero to the timing of the disappearing the snow cover. It is thought that the heat flux for melting in last April is overestimated against the real value. On the other hand, the simulated snow depth is also greater than observed one corresponding to the difference of SWE. Now we could implement the new water channel process because we

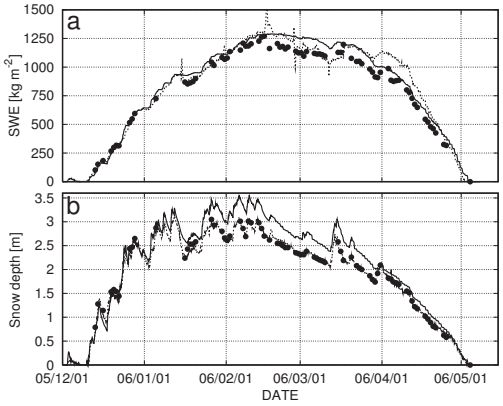

Figure 4: The observed and simulated a)SWE and b)snow depth. Solid lines, points and dash lines correspond to simulated, manually observed and automatically observed ones.

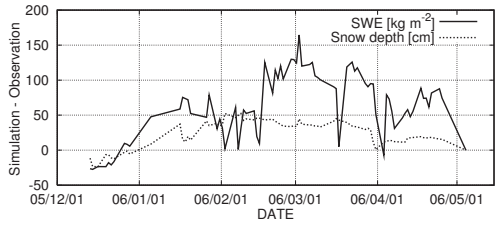

Figure 5: The difference of SWE and the snow depth between simulated and manually observed ones. Solid line: SWE (kg m^{-2}), dash line: snow depth (cm)

obtained comparably good results on the mass balance against past works.

We showed the observed and simulated fractions of the thickness with the wet grains F_w in Figure 6. The simulated F_w are calculated with the S_t over the range of 0.071-0.074. As mentioned below in the explanation of Figure 8, F_w with the pit observation includes the layers of "wet grains/rounded grains" and exclude "rounded grains/wet grains" as the layer with the wet grains to calculate the equation (27).

In Figure 6, the curves of F_w become different results according to a small changes of S_t. When the threshold S_t is 0.073, we obtain a better estimation of F_w compared with others until 15 February. Then we decided to employ this value 0.073for the threshold of the water channel switch. F_w with the pit observation kept in the value ranging from about 0.5 to 0.8. in the period from 24 February to 24 March although F_w with the model increased and become greater than the F_w with the pit observation. We thought that this disagreement is caused by other processes of the water channel which are ignored above.

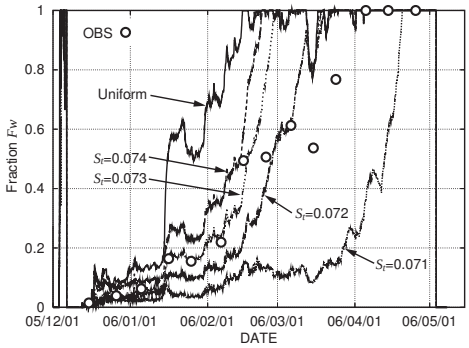

Figure 6: Time series of F_w. Solid line indicates the simulated F_w with the uniform condition, dash lines indicate F_w with each threshold values and points indicate F_w with the pit observations.

The reasons of these results are described in detail later. The selected value of threshold S_t is slightly small compared with the irreducible liquid water saturation S_{wi} =0.07. It means that the infiltration of the uniform condition only occur at the state of the liquid water saturation ranging from 0.07 to 0.073, which is not likely to occur.

The time series of the layer structure obtained from the pit observations are shown in Figure 7 a), and from the simulations is showed in Figure 7b) with the uniform conditions and c) with the water channels. The detail of the pit observations and the simulated vertical structures of the snow layers on a) 16 January, b) 6 February, c) 24 February and d) 6 March are shown in Figure 8. Each figure includes three figures which indicate the pit observation in left hand side (obs.), the simulated result with the uniform condition in center (cal.1) and the simulated result with the water channel in right hand side (cal.2). The "wet grains / rounded grains" means the snow type of the wet grains partially including the rounded grains together. The "rounded grains/wet grains" means snow type of the rounded grains partially including the wet grains together. From Figure 7 and 8, although the thickness and the position of each layer are a little different, we obtained good results of the vertical structure in the snowpack.

It is also found that the structures until 15 February with the water channel are successively performed. Moreover, the results including the rainfall event, which occurred four times (32mm in 14-15 January, 18mm in 30 January-3 February, 16mm in 7-8 February and 37mm in 14-17 February) seems to be well simulated until 15 February. Takeuchi et al. (2006) observed the water channel due to the rainfall at 14-15 January in the rounded grains layer in 16 January. It is thought that L2 indicated in Figure 8 a is

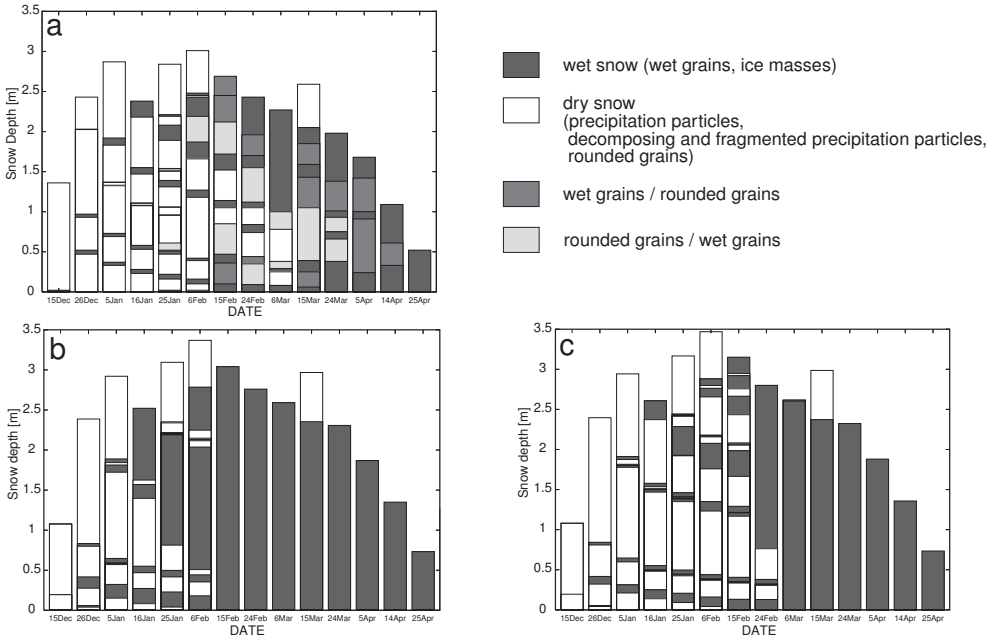

Figure 7: The time series of the simplified layer structures of the snowpack of a) the pit observation, b) simulation with uniform condition (cal.1) and c) simulation with water channel (cal.2)

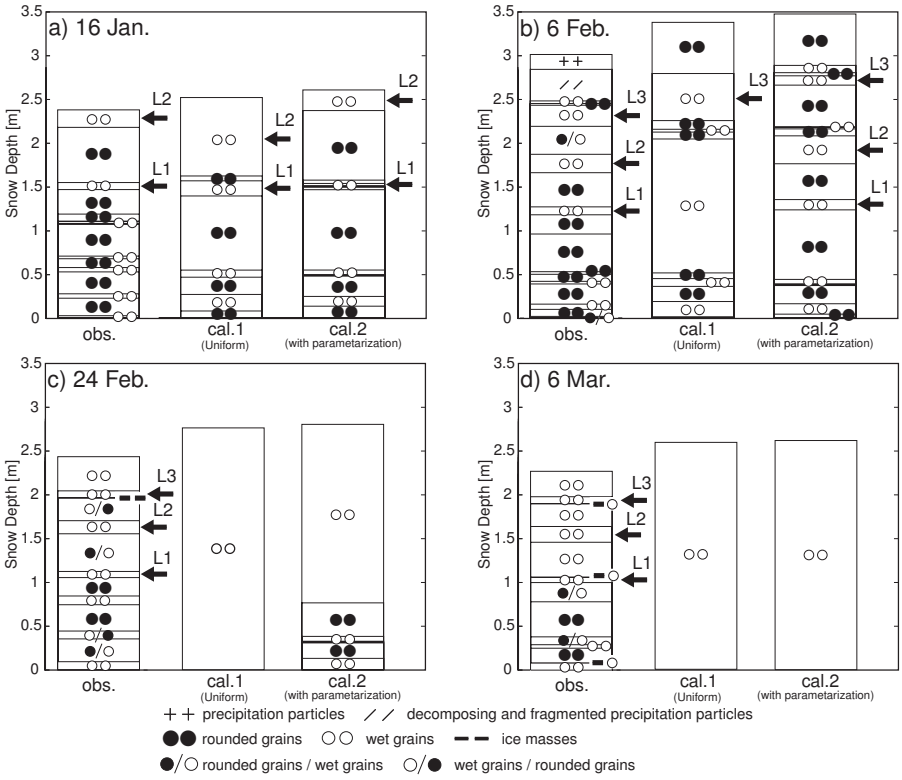

Figure 8: The layer structures of the snowpack on a) 16 Jan. 2006, b) 6 Feb 2006, c) 24 Feb. 2006 and d) 6 Mar. 2006 (left: pit observation, center: with uniform condition (cal.1), right: with water channel (cal.2)).

the layer generated by the water channel at 14 January. The simulated result with the water channel in Figure a (cal.2) shows L2 layer as same as the pit observation. It suggests that the new water channel model take a good role to form the water channel. But, in the uniform condition shown in Figure 8 a (cal.1), we obtain thicker L2 layer than L2 in the pit observation. The layer, named L3 in Figure 8, is formed by the rainfall on 30 January-3 February. It is almost the same result as L2.

After 24 February, the uniform infiltration becomes dominant and all layers in the snowpack become to the snow type of the wet grains in the both case of the simulation (Figure 8 c) though the pit observation shows the different result. The observed positions of the wetting front are the wet grains layer L2 on 24 February, and the wet grains layer L1 on 6 March, 15 March and 24 March (Figure 7 and 8 c, d). It is thought that these wetting fronts located at the L1 and L2 in the pit observations act a role of the impermeable layer even in the melting season.

We have already explained the three conditions to form the preferential flow in the snowpack (1. Introduction). And we employ only one condition mentioned as 3). Although the selected value of S_t may not be favorable for the simulation in the melting season, It is thought that the problem on the formation of the wetting front in the melting season mentioned above is related to the condition 1) and 2). The case on 24 February is not identified whether the conditions of 1) or 2) because we do not also identified the position of the impermeable layer above/below the wet grains L2. At first of two cases, if the impermeable layer would locate above L2, It would be under the condition 1) which needs to consider the change of the S_w - P_c curve according to the snow type. If the impermeable layer located in under this wet grains layer (L2), it is assumed that the impermeable layer is formed in the wetting front into dry snow that we consider in model. At the second case, if the impermeable layer would locate below L2, It would be under the condition 3), which should be select S_t exactly, i.e. a consideration of the changing the value with the snow property.

On the other hand, on 6 March shown in Figure 8 d), the position of the impermeable layer can be identified and it is found that the wet grains layer L1 is under the condition 2) where the impermeable is formed from the ice layer above the wet grains. This ice layer generated just before 6 March seems to be formed by the capillary barrier at the fine over the coarse texture before the infiltration water is intercepted and freeze at this layer. Once the ice layer is formed, the impermeable ability of the ice layer continues during some period. Then, it is thought that the dry snow layer below the ice layer maintains in the snowpack during about one month.

As the result, though we obtain the successful result to implement the new water channel process, it is suggested that the condition 1) and 2) need to be considered to perform more accurate simulations

5. CONCLUSION

New water channel numerical process for the multiple snow layer model to parameterize the limitation of the channel flow with the liquid water content was developed and validated during winter 2005/06 at Tohkamachi, Japan where the liquid precipitation often occur in middle winter. The conceptual procedure to generate the water channel is followed on the study of Nohguchi (1984). This model is taken into account of the water infiltration down to the dry snow. It is not considered to the impermeable processes by the ice layer (Gerbel,1954; Langham,1974; Marsh and Woo,1984a, 1984b) and the fine textured layer over the coarse one (Wakahama,1963; Waldner et al.,2004). We controlled the vertical water flux just above the dry snow by the limiter which was expressed with the threshold value of the liquid water content and removed the water to infiltrate along the water channel at the occurred position as the immediate downward flow. And we performed the comparison between the pit observation and the simulated results.

First of all, we had good results of simulations about the snow water equivalent and the snow depth compared with the pit observations. The water mass balance of the snowpack also seems to be good for doing the following study of the infiltration process.

It is found that the new water channel process implemented in this study worked well applying the rainfall event in middle winter, and the comparison of the vertical structure in the snowpack between the pit observations and simulated results showed that the simulation with the water channel was more successively done than that with the uniform infiltration especially until 15 February. On the other hand, we did not simulate the dry snow remained after 24 February in the pit observation, which may result in the other case of the forming the water channel; e.g. the ice layer and the fine textured layer above the coarse one.

6.REFERENCE

Brun, E., 1989. Investigation on wet-snow metamorphism in respect of liquid-water content. Ann. Glaciol. 13, 22-26.

Brun, E., Martin, E., Siomn, V., Gendre, C., Coléou, C., 1989. An energy and mass model of snow cover suitable for operational avalanche forecasting. J. Glaciol. 35(121), 333-342

Brun, E., David, P., Sudul, M., Brunot, G., 1992. A numerical model to simulate snow-cover stratigraphy for operational avalanche forecasting. J. Glaciol. 38(128), 13-22.

Colbeck, S.C., 1972. A theory of water percolation in snow. J. Glaciol. 11(63), 369-385.

Colbeck, S. C., 1974. The capillary effects on water percolation in homogeneous snow. J. Glaciol. 13(67), 85-97.

Colbeck, S. C., 1979. Water flow through heterogeneous snow. Cold Reg. Sci. Technol. 1(1), 37-45.

Colbeck, S. C., Anderson, E. A., 1982. The permeability of melting snow cover. Water Resources Research 18(4), 904-908.

Coléou, C., Lesaffre, B., 1998. Irreducible water saturation in snow: experimental results in cold laboratory. Ann. Glaciol. 26, 64-68

Coléou, C., Xu, K., Lesaffre, B., Brzoska JB., 1999. Capillary rise in snow. Hydrol. Process. 13, 1721-1732

Gerbel, R.W., 1954. The transmission of water through snow. Transactions American Geophysucal Union 35(3), 475-485.

Gustafsson, D., Waldner, P., Stähli, M., 2004. Factors governing the formation and persistence of layers in a subalpine snowpack. Hydrol. Process. 18, 1165-1183.

Hirai, M., Sakashita, T., Kitagawa, H., Tsuyuki, T., Hosaka, M., Oh'izumi M., 2007. Development and validation of a new land surface model for JMA's operational global model using the CEOP observation dataset. J. Meteor. Soc. Japan. 85A,1-24.

Illangasekare, T.H., Rodney, J., Walter, J., Meirer, M.F., Pfeffer, W.T., 1990. Modeling of meltwater infiltration in subfreezing snow. Water Resour. Res. 26(5), 1001-1012.

Jordan, P., 1983. Meltwater movement in a deep snowpack 1. Field Observations. Water Resour. Res. 19(4), 971-978.

Jordan, R., 1991. A one-dimensional temperature model for a snow cover. U.S. Army Corps of Engineers, Cold Regions Research & Engineering Laboratory, Special Report 91-16.

Kajikawa, M., 1989. Relationship between new snow density and shape of snow crystals. Seppyo 51(3), 178-183.

Kinosita, S., 1963. Compression of snow immersed in water of 0℃. Ⅰ. Low Temp. Sci. Ser. A 21,13-22.

Kumakura, T., Yamanoi, K., Hayakawa, N., 2004. Comparision between observed and calculated snow depths using a multi-layer snow densification model in Hokuriku. Seppyo 66(1), 35-50.

Lagham, E.J., 1974. Phase equilibria of veins in polycrystalline ice. Can. J. Earth Sci. 11, 1280-1287.

Lehning, M., Bartelt, P., Brown, B., Russi, T., Stöckli, U., Zimmerli, M., 1999. SNOWPACK model calculations for avalanche warning based upon a new network of weather and snow stations. Cold Reg. Sci. Technol. 30, 145– 157.

Marsh, P., Woo, M.K., 1984a., Wetting front advance and freezing of meltwater within a snow cover 1. Observations in the Canadian arctic. Water Resour. Res., 20(12), 1853-1864.

Marsh, P., Woo, M.K., 1984b., Wetting front advance and freezing of meltwater within a snow cover 2. A simulation model., Water Resour. Res. 20(12), 1865-1874.

Nohguchi, Y., 1984. Formation of dimple-pattern on snow Ⅰ. Report of the National Research Institute for Earth Science and Disaster Prevention 33, 237-254.

Shimizu H. 1970. Air permeability of deposited snow. Cont. Inst. of Low Temp. Sci. Ser. A 22, 1-32.

Sonntag, D., 1994. Advancements in the field of hygrometry. Meteorol. Z. 3, 51-66.

Sugie, S., Naruse, R., 2000. Measurements of unsaturated hydraulic conductivity of snow. Seppyo 62(2),117-127.

Takeuchi, Y., Endo, Y., Murakami, S., Niwano, S., 2007. Characteristics of snow hardness at Tohkamachi during the winter of 2005-06. Seppyo 69(1), 61-69.

Tusima K., 1978. Grain coarsening of ice particles immersed in pure water. Seppyo 40(4), 155-165.

Wakahama, G., 1963. The infiltration of melt water into snow cover Ⅰ. Low Temp. Sci. Ser. A 21, 45-74.

Yamanoi, K., Endo, Y., Kominami, Y., Niwano, S., Ohzeki, Y., 2000. Meteorological statistics during the past 80 years in Tohkamachi city, Niigata (1918~1997). Bull. For. & For. Prod. Res. Inst. 377, 61-99.

Yokoyama, K., Ohno, H., Kominami, Y., Inoue, S., Kawakata, T., 2003. Performance of Japanese precipitation gauges in winter. Seppyo 65(3), 303-316.